Catalysis Communications 31 (2013) 66–70

Contents lists available at SciVerse ScienceDirect

Catalysis Communications

journal homepage: www.elsevier.com/locate/catcom

Short Communication

Influence of Ti–O–Si hetero-linkages in the photocatalytic degradation of Rhodamine B

Shivatharsiny Rasalingam [a], Harrison S. Kibombo [a], Chia-Ming Wu [a], Sridhar Budhi [a], Rui Peng [a], Jonas Baltrusaitis [b], Ranjit T. Koodali [a,*]

[a] Department of Chemistry, University of South Dakota, Vermillion, USA
[b] PhotoCatalytic Synthesis Group, University of Twente, The Netherlands

ARTICLE INFO

Article history:
Received 30 October 2012
Received in revised form 13 November 2012
Accepted 16 November 2012
Available online 23 November 2012

Keywords:
Titania, Silica
Mixed oxide
Surface characterization
Photocatalysis

ABSTRACT

The influence of Ti–O–Si hetero-linkages in the degradation of Rhodamine B (RhB) dye over TiO_2–SiO_2 xerogels is exemplified by XPS analysis. We demonstrate a relationship between the percentage surface content of Ti–O–Si and the rate of photocatalytic degradation of RhB. Our detailed surface investigation revealed that the overall degradation of RhB is enhanced due to the high surface percentage content of Ti–O–Si species, high crystallinity of titania phase, and its effective dispersion on a high surface area porous silica support.

1. Introduction

The degradation of organic pollutants has gained significant attention in recent years. TiO_2 has been widely used as a photocatalyst for this purpose. However, it is limited in application due to low surface area and hydrophobicity, [1] but these factors may be overcome by modification with silica, [2,3] zeolites, Al_2O_3 etc. [4]. In addition, the large band gap is a big limitation that can be overcome by use of novel photocatalysts [5–8]. Rhodamine B (RhB) degradation studies have been explored using TiO_2–SiO_2 xerogels under UV [9,10] and visible [11] light irradiation with the activity mainly credited to enhanced crystallinity of the titania phase.

Ti–O–Si heterolinkages (in TiO_2–SiO_2) have been implicated for enhanced photoefficiencies, however, the commonly acclaimed IR evidence of a Ti – O – Si bond appearing in the range of 930–965 cm^{-1} is not compelling since bands due to Si–O–H groups also appear in the same region [12]. Here, we demonstrate a clear relationship between the percentage surface content of Ti–O–Si and the rate of photocatalytic degradation of RhB.

2. Experimental

2.1. Preparation

In a typical procedure, the TiO_2–SiO_2 xerogels were prepared by adding solvent (ethanol), co-solvent of choice (hexane, toluene, or *p*-xylene), tetraethyl orthosilicate, water, and conc. HNO_3 in a beaker at room temperature. These samples are labeled as TSX1, TSX2, TSX3, and TSX4 respectively. Then, $Ti(^iOPr)_4$ was added to obtain a TiO_2:SiO_2 molar ratio of 1:1. The gel was dried and calcined in air at 550 °C [13]. More details are provided in the supplementary section.

2.2. Characterization

Powder X-ray diffraction patterns were recorded on a Rigaku Ultima IV instrument. Nitrogen physisorption studies were carried out using Quantachrome NOVA 2200*e* instrument. Diffuse Reflectance Spectroscopy (DRS) was carried out by using a Cary 100 Bio UV–vis spectrophotometer equipped with a Harrick DR accessory. TEM images were recorded on a Tecnai G^2 instrument operating at 120 kV. X-ray Photoelectron Spectroscopy (XPS) studies were carried out using a custom-designed Kratos Axis Ultra system. More details are available in the supplementary section.

2.3. Photocatalytic activity

Photocatalysis experiments were carried out as described previously [14]. Briefly, 25 mg of photocatalyst was dissolved in 50 mL of RhB solution (2×10^{-5} M) in a quartz reactor. The suspensions were stirred in the dark for 30 min to ensure adsorption–desorption equilibrium. The reaction temperature was maintained at 25 °C. Irradiation was carried out by using a Xe lamp (Newport 1000 W) through a cut off filter to eliminate light of wavelengths below 420 nm. After irradiation, the suspensions were centrifuged and the amount of RhB remaining in

* Corresponding author. Tel.: +1 605 677 6189; fax: +1 605 677 6397.
E-mail address: Ranjit.Koodali@usd.edu (R.T. Koodali).

1566-7367/$ – see front matter © 2012 Elsevier B.V. All rights reserved.
http://dx.doi.org/10.1016/j.catcom.2012.11.016

solution was analyzed by UV–vis spectroscopy by monitoring its absorbance at the maximum wavelength of 554 nm.

2.4. Adsorption studies

20 mg of photocatalyst was added to 20 mL of aqueous RhB in amber bottles. The resultant suspensions were stirred at 300 rpm at room temperature (25 ± 2 °C) in the dark for 14 h to ensure adsorption–desorption equilibrium. The suspension was centrifuged and the equilibrium concentration of RhB was calculated as described previously. More details are indicated in the supplementary section.

3. Results and discussion

Powder XRD results are shown in Fig. 1. Titania–Silica Xerogel prepared in ethanol (TSX-1) show a broad peak of low diffraction contrast due to the amorphicity of silica and/or effective dispersion of small anatase crystallites. The use of hexane results in a material (TSX2) that exhibit crystalline phases of anatase. The introduction of aromatic non-polar co-solvents such as toluene (TSX3) and *p*-xylene (TSX4) resulted in more intense peaks due to the anatase phase suggesting an improvement in crystallinity. The physisorption properties were investigated and the xerogels exhibited Type IV isotherms [15,16] characteristic of mesoporous materials (Fig. S1). TSX1 exhibited the lowest surface area. The pore sizes of the xerogels were found to be nearly 36 Å. Narrow pore size distributions and larger surface areas were obtained for xerogels prepared using hexane, toluene, and *p*-xylene as co-solvents. The role of solvents in tuning the porosities is not the focus of this investigation; however to provide clarity to the reader, some details are provided in the supplementary section.

The DRS spectra were converted to Tauc plots via the Kubelka–Munk function as shown in Fig. 2 and indicate band gaps of TiO_2 to be between 3.18 and 3.24 eV. TEM image (Fig. S2) suggests high porosities in the mixed oxides.

Quantitative XPS studies were employed to determine the chemical and electronic state of surface Ti and oxygen atoms, and were fundamental to the elucidation of the structure–activity relationship. The survey spectra (Fig. S3) indicate 2 peaks due to Ti $2p_{3/2}$ and Ti $2p_{1/2}$ spin–orbital splitting photoelectrons, within 458.4–458.8 and 464.4–464.5 eV (similar to anatase [17]). The peak separation between the Ti 2p signals is ~5.7 eV and in agreement with previous reports [18]. The O 1s spectra are shown in Fig. 3. The low binding energy (B.E.) observed near 529.7–530.2 eV is ascribed to bulk O^{2-} in anatase (Ti–O–Ti) which is in agreement with previous report [19]. The high energy band in the range of 532.1–532.3 eV is due to Si–O–Si. The percentage surface content of Ti–O–Ti, Ti–O–H, Ti–O–Si, Si–O–Si, and Si–O–H was calculated as described as follows and the results are indicated in Table 1. The O 1s transition was first fit to two peaks near 530 eV [19] and 532 eV [20] as stated previously. De-convolution of the broad band's between 530 and 532 eV led to three additional peaks. The band at 531.3 eV is due to Ti–O–H species [19,21], while the band near 531.7 eV is due to Ti–O–Si species [18,19,22], and that near 532.7 eV is ascribed to Si–O–H [20] as indicated in these reports. All of the peaks used for quantification were Gaussian/Lorentzian shape GL (30:70) curves with equivalent eV at the full-width-half-maximum (fwhm). In order to normalize for the differences in specific surface areas (SSA), these percentages were multiplied by the SSA to obtain apparent surface coverages (ASC). The accuracy in binding energy (B.E.) values is estimated to be 0.1 eV.

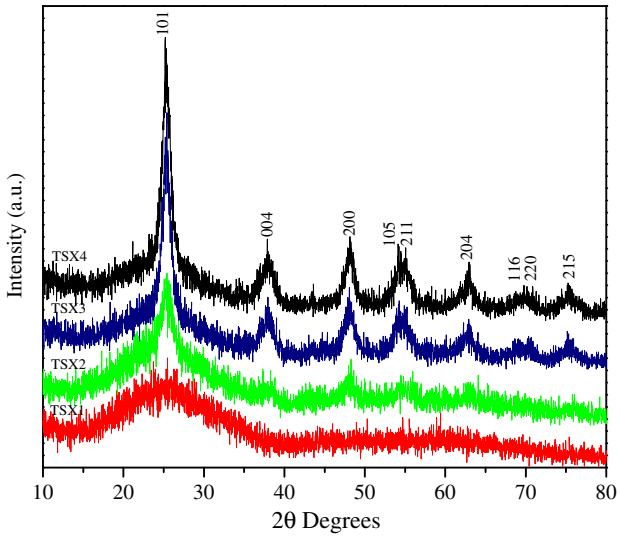

Fig. 1. Powder X-ray diffraction patterns of TiO_2–SiO_2 xerogels.

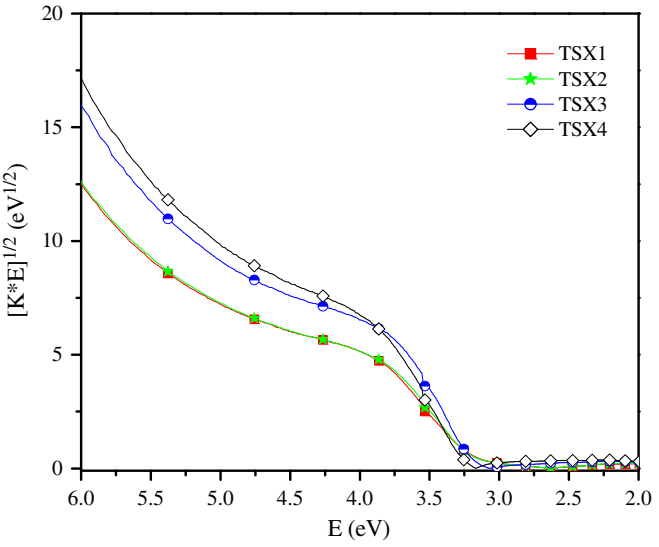

Fig. 2. Tauc plots of TiO_2–SiO_2 xerogels.

RhB dye molecules are degraded efficiently under visible light irradiation. An extensive study detailing the photooxidation pathways is presented by Hidaka and co-workers [23]. The xerogels studied obey pseudo first-order kinetics and the apparent rate constant (k_{app}) was calculated from the plot of relative concentration vs. time as shown in Fig. 4. Our results indicate that the amount of RhB adsorbed in the xerogels evaluated for photocatalytic degradation was minimal (less than 2%) and thus kinetic measurements for these samples were performed under conditions in which only a small fraction of the substrate was adsorbed. Since we are comparing relative trends within a set of samples (that exhibited similar adsorptive properties in the dark), the apparent rate constants (k_{app}) obtained assuming pseudo-first order kinetics may be used as rough guide to assess the photoactivity among different photocatalysts as recognized by Langford and co-workers [24]. The degradation rates differ with TSX1 showing the least activity in comparison to TSX4 that exhibits the highest activity.

We noticed a good correlation of the overall degradation rates with the specific surface areas of the xerogels. Since the xerogels studied were of equimolar oxide ratio (TiO_2:SiO_2 = 1:1), the variation in photocatalytic activity necessitated a probe into the actual factor(s) responsible for the differences in the activities. The close proximity in value of oxide content and pore sizes minimizes differences due to diffusion effects and permits a realistic comparison. The results obtained are summarized in Table 2. TSX1 with low surface area (7 $m^2\ g^{-1}$) showed $k_{app} = 7.4 \times 10^{-5}\ s^{-1}$. An increment in

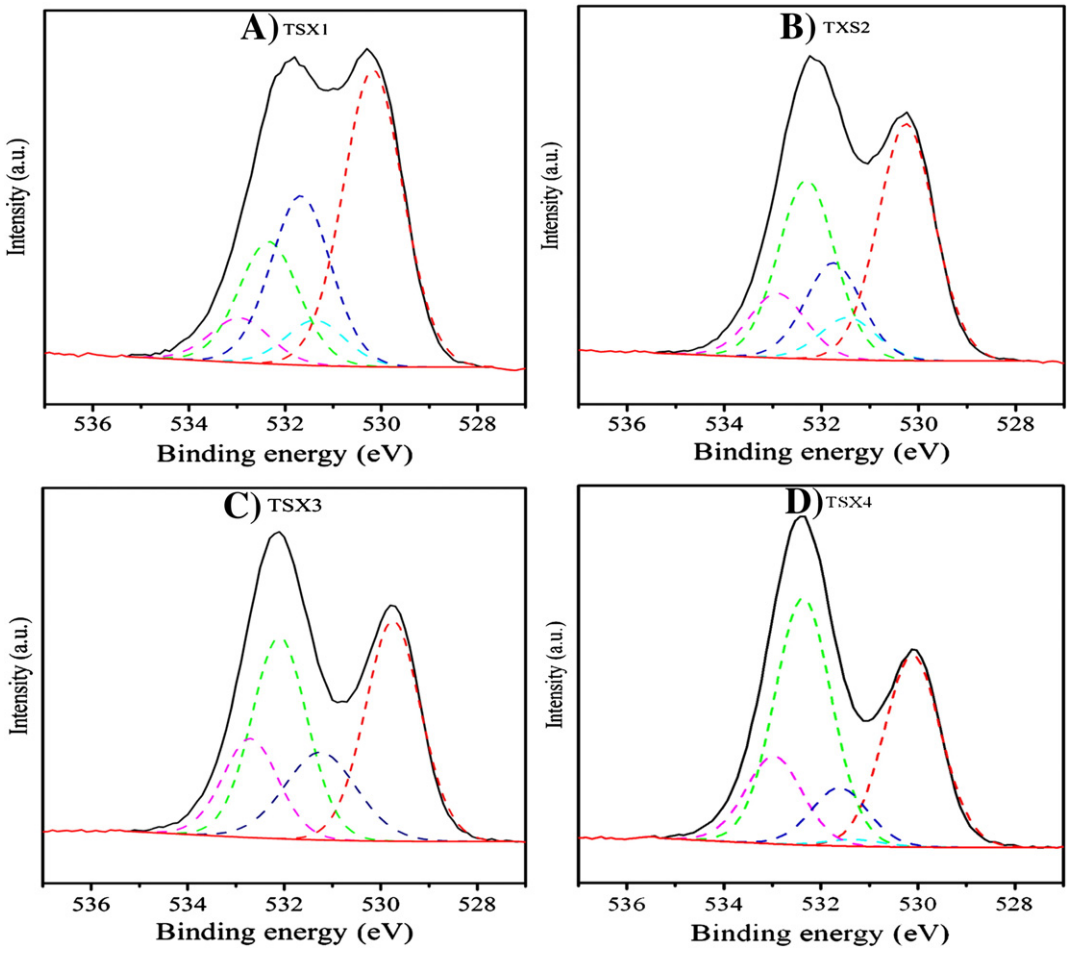

Fig. 3. XPS spectra of deconvoluted O 1s spectra of (A) TSX1, (B) TSX2, (C) TSX3, and (D) TSX4.

surface area to 88, 125, and 363 $m^2\ g^{-1}$ resulted in a marked increment in k_{app} of 2.48, 6.09, and $8.65\times10^{-4}\ s^{-1}$ for TSX2, TSX3, and TSX4 respectively.

XPS analysis provided detailed information regarding the role of the active surface species. In this study, we do not see a direct correlation between the % surface content of Ti–O–H groups and the degradation rate (see Tables 1 and 2). FT-IR studies (Fig. S4) indicate a band near 960 cm^{-1} that is believed to be due to Ti–O–Si linkages. However pure silica shows a very broad band near 975 cm^{-1} due to Si–O–H groups that partly overlaps with the band near 960 cm^{-1} making it difficult to unambiguously prove the existence of Ti – O – Si bonds from IR studies [25]. The intensity of the band at 960 cm^{-1} for the four xerogels appears comparable. Also, the maximum adsorption capacity (q_m~2×10^{-5} mol.g^{-1}) calculated using the Langmuir equation seems similar for all 4 xerogels (Table 3) and thus the differences in photocatalytic activities may be attributed to other factors. This observation prompted a detailed investigation into the surface properties. Messina and Schulz have reported that q_m of dyes on titania–silica have a direct correlation with pore diameters rather than surface areas as we have seen [26].

Sol–gel reactions consist of hydrolysis and condensation processes that ultimately result into bond breaking of $Ti(^iOPr)_4$ and TEOS to form Ti–O–Si heterolinkages. Since the titania amount is similar, this suggests that the differences in activities are due to variations in the apparent surface coverage (ASC) of Ti–O–Si that emerges as a key factor as calculated and described on page 3 in the supplementary section. TSX1 exhibits the lowest degradation rate constant ($7.4\times10^{-5}\ s^{-1}$) owing to the low ASC of Ti–O–Si of 1.7. Likewise, for TSX4, the ASC of 35.7 renders this xerogel as the most active photocatalyst ($8.65\times10^{-4}\ s^{-1}$). For comparison, we have prepared pure titania under similar conditions and obtained surface area of 32 $m^2\ g^{-1}$ and $k_{app}=3.4\times10^{-4}\ s^{-1}$. The activity of pure titania is higher than TSX1 and TSX2 mainly due to the high crystallinity that acts as the overriding factor in minimizing charge carrier recombination and enhancing photocatalytic efficiency. Yet despite its high crystallinity, its activity is lower than TSX3, or TSX4. However, one should exercise

Table 1
O 1s binding energies (B.E.) and fwhm of core electrons for TiO_2–SiO_2 xerogels.

Xerogel	O 1s B.E. (eV)					% Surface content				
	Ti–O–Ti	Ti–O–H	Ti–O–Si	Si–O–Si	Si–O–H	Ti–O–Ti	Ti–O–H	Ti–O–Si	Si–O–Si	Si–O–H
TSX1	530.2	531.4	531.7	532.3	532.9	43.8	6.7	24.9	18.0	6.6
TSX2	530.2	531.4	531.7	532.3	532.9	38.3	6.8	15.6	28.8	10.5
TSX3	529.7	none	531.2	532.1	532.7	34.8	0	17.9	31.7	15.6
TSX4	530.1	531.3	531.6	532.3	532.9	32.5	1.1	9.8	41.7	14.9

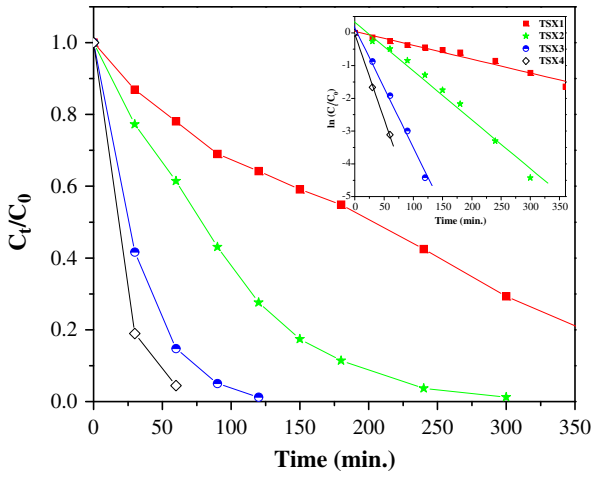

Fig. 4. Plots of C_t/C_0 vs. time and inset $\ln(C_t/C_0)$ vs. time for TiO_2–SiO_2 xerogels.

Table 2
Textural properties and the dye degradation rate constants of TiO_2–SiO_2 xerogels.

Xerogel	CS	S:CS	SSA (m^2/g)	ASC (m^2/g)	k_{app} (10^{-4}, s^{-1})
TSX1	Ethanol	1:0	7	1.7	0.74
TSX2	Hexane	1:1	88	13.7	2.48
TSX3	Toluene	1:1	125	22.4	6.09
TSX4	*p*-Xylene	1:1	363	35.7	8.65

TSX refers to TiO_2–SiO_2 xerogel. The TiO_2:SiO_2 molar ratio is 1:1. S:CS is the volume ratio of solvent (ethanol) to co-solvent. SSA refers to specific surface area. ASC is the Apparent Surface Coverage of Ti–O–Si species and k_{app} is the photocatalytic pseudo first-order degradation rate constant.

caution in comparing titania with titania–silica since differences in crystallinities, porosities, and dispersion vary. Our results suggest that the dye photodegradation rate is dependent on the ASC of the Ti–O–Si phase. The presence of Ti–O–Si phase has been hypothesized to be favorable for photocatalytic reactions [4] but this study provides a clear correlation. In our xerogels, the titanium ions are in octahedral coordination and the titania domains coordinate to silica via surface silanol groups. This generates non-balanced oxygen atoms due to differences in the coordination of Si and Ti [27]. The increased photoactivity is attributed to the presence of Ti–O–Si phase (at the TiO_2–SiO_2 interface) that serves to activate the oxidation of organics [4]. The presence of the photoactive titania phase in close proximity to the TiO_2–SiO_2 interface results in enhanced photocatalytic activities via the reaction of oxidizing intermediates such as hydroxyl radicals that are generated at the titania sites and believed to be the most active oxidative species for degradation. The increased activity is due to the presence of the mixed TiO_2–SiO_2 at the interphase region. We also acknowledge that the high activity of TSX4 may be due to the higher crystallinity of the titania phase in comparison to TSX1. The peaks due to the amorphous phase of silica coincide with that of the titania phase and we cannot with surety compare the relative crystallinity of titania in the four xerogels; however it seems that the crystallinities of the titania phases in the xerogels, TSX3 and TSX4 are comparable and the differences in activity may thus be primarily due to the higher amount of mixed Ti–O–Si phase in TSX4. Thus, the combination of higher ASC of Ti–O–Si phase, high crystallinity, and the effective dispersion of the photoactive titania phase is responsible for the high activity of TSX4.

Preliminary results with phenol and 4-cholorophenol also suggest similar trends suggesting the important role of Ti–O–Si heterolinkages in photocatalytic degradation of organics but a detailed study is under progress and is beyond the purview of this paper.

Table 3
Adsorption data for titania–silica xerogels.

Xerogel	q_m (mol g^{-1})	R^2
TSX1	2.20×10^{-5}	0.999
TSX2	2.16×10^{-5}	1.000
TSX3	2.72×10^{-5}	0.992
TSX4	2.09×10^{-5}	1.000

TSX refers to TiO_2–SiO_2 xerogel. The TiO_2:SiO_2 molar ratio is 1:1. The maximum amount of adsorption (q_m) was calculated using Eq. (1):

$$\frac{1}{q_e} = \left(\frac{1}{K_L q_m}\right)\frac{1}{C_e} + \frac{1}{q_m}.$$

4. Conclusion

In conclusion, TiO_2–SiO_2 xerogels were prepared and our detailed surface investigation revealed that the photocatalytic degradation of RhB is enhanced due to the high surface content of Ti–O–Si species, high crystallinity of titania phase, and its effective dispersion on a high surface area porous silica support. We believe that this work bridges this gap in the existing literature by providing quantitative insight into the role of Ti–O–Si heterolinkages and its influence on the photocatalytic activity. The increased activity is due to this interphase region.

Acknowledgments

We extend sincere gratitude to NSF-CHE-0722632, NSF-EPS-0903804, DE-EE0000270, SD NASA-EPSCOR NNX12AB17G and the State of South Dakota. We also deeply thank Prof. V. H. Grassian for her assistance with XPS instrumentation.

Appendix A. Supplementary data

Supplementary data to this article can be found online at http://dx.doi.org/10.1016/j.catcom.2012.11.016.

References

[1] M.D. Hernandez-Alonso, F. Fresno, S. Suarez, J.M. Coronado, Energy & Environmental Science 2 (2009) 1231–1257.
[2] H.S. Kibombo, R. Peng, S. Rasalingam, R.T. Koodali, Catalysis Science & Technology 2 (2012) 1737–1766.
[3] C. Anderson, A.J. Bard, The Journal of Physical Chemistry 99 (1995) 9882–9885.
[4] C. Anderson, A.J. Bard, The Journal of Physical Chemistry. B 101 (1997) 2611–2616.
[5] R. Asahi, T. Morikawa, T. Ohwaki, K. Aoki, Y. Taga, Science 293 (2001) 269–271.
[6] Y. He, L. Zhao, Y. Wang, T. Li, T. Wu, X. Wu, Y. Wu, Industrial and Engineering Chemistry Research 50 (2011) 7109–7119.
[7] Y. Wang, Y. He, T. Li, J. Cai, M. Luo, L. Zhao, Catalysis Communications 18 (2012) 161–164.
[8] T. Li, L. Zhao, Y. He, J. Cai, M. Luo, J. Lin, Applied Catalysis B: Environmental 129 (2013) 255–263.
[9] J.B. Joo, Q. Zhang, I. Lee, M. Dahl, F. Zaera, Y. Yin, Advanced Functional Materials 22 (2012) 166–174.
[10] P. Wilhelm, D. Stephan, Journal of Photochemistry and Photobiology A: Chemistry 185 (2007) 19–25.
[11] Q. Zhang, D.Q. Lima, I. Lee, F. Zaera, M. Chi, Y. Yin, Angewandte Chemie 123 (2011) 7226–7230.
[12] O. Alaoui, Q. Nguyen, T. Rhlalou, Environmental Chemistry Letters 7 (2009) 175–181.
[13] S. Budhi, H.S. Kibombo, D. Zhao, A. Gonshorowski, R.T. Koodali, Materials Letters 65 (2011) 2136–2138.
[14] J. Becker, K.R. Raghupathi, J. St Pierre, D. Zhao, R.T. Koodali, Journal of Physical Chemistry C 115 (2011) 13844–13850.
[15] R. Mariscal, M. López-Granados, J.L.G. Fierro, J.L. Sotelo, C. Martos, R. Van Grieken, Langmuir 16 (2000) 9460–9467.
[16] M. Kruk, M. Jaroniec, Chemistry of Materials 13 (2001) 3169–3183.
[17] X. Gao, S.R. Bare, J.L.G. Fierro, M.A. Banares, I.E. Wachs, The Journal of Physical Chemistry. B 102 (1998) 5653–5666.
[18] M.J. Kim, K.-D. Kim, H.O. Seo, Y. Luo, N.K. Dey, Y.D. Kim, Applied Surface Science 257 (2011) 2489–2493.

[19] B. Erdem, R.A. Hunsicker, G.W. Simmons, E.D. Sudol, V.L. Dimonie, M.S. El-Aasser, Langmuir 17 (2001) 2664–2669.
[20] M. Fukushima, Y. Zhou, Y.-I. Yoshizawa, K. Hirao, Journal of the European Ceramic Society 28 (2008) 1043–1048.
[21] D. Sun, Y. Huang, B. Han, G. Yang, Langmuir 22 (2006) 4793–4798.
[22] J. Wang, X. Liu, R. Li, P. Qiao, L. Xiao, J. Fan, Catalysis Communications 19 (2012) 96–99.
[23] F. Chen, J. Zhao, H. Hidaka, International Journal of Photoenergy 05 (2003) 209–217.
[24] Y. Xu, C.H. Langford, Langmuir 17 (2001) 897–902.
[25] R.J. Davis, Z. Liu, Chemistry of Materials 9 (1997) 2311–2324.
[26] P.V. Messina, P.C. Schulz, Journal of Colloid and Interface Science 299 (2006) 305–320.
[27] M. Itoh, H. Hattori, K. Tanabe, Journal of Catalysis 35 (1974) 225–231.